Network structure of the human musculoskeletal system shapes neural interactions on multiple timescales

Jennifer N. Kerkman[a], Andreas Daffertshofer[a], Leonardo Gollo[b], Michael Breakspear[b,c], Tjeerd W. Boonstra[b,d,1]

[a]Faculty of Behavioural and Movement Sciences, Vrije Universiteit Amsterdam, Amsterdam, the Netherlands

[b]QIMR Berghofer Medial Research Institute, Brisbane, Australia

[c]Metro North Mental Health Service, Brisbane, QLD, Australia

[d]Black Dog Institute, University of New South Wales, Sydney, Australia

[1] Corresponding author

Tjeerd Boonstra, Black Dog Institute, Hospital Rd, Sydney NSW 2031, Australia. Email: t.boonstra@unsw.edu.au

Abstract

Human motor control requires the coordination of muscle activity under the anatomical constraints imposed by the musculoskeletal system. Interactions within the central nervous system are fundamental to motor coordination, but the principles governing functional integration remain poorly understood. We use network analysis to investigate the relationship between anatomical and functional connectivity amongst 36 muscles during postural tasks. We find a modular structure of functional networks that is strongly shaped by the anatomical constraints of the musculoskeletal system. Muscle networks exhibit a multilayer architecture with distinct spectral fingerprints in which functional interactions are established across multiple timescales. Changes in postural tasks are associated with a reconfiguration in the coupling between functional modules. These results identify a distributed neural circuitry in which parallel pathways give rise to different functional modes that facilitate flexible motor behaviours. This multi-level network approach to the motor system offers a unique window into the neural basis for human movement.

Introduction

The human body is a complex system consisting of many subsystems and regulatory pathways. The musculoskeletal system gives the body structure and creates the ability to move. It is made up of more than 200 skeletal bones, connective tissue and over 600 skeletal muscles[1]. Muscles are attached to bones through tendinous tissue and can generate movement around a joint when they contract. The central nervous system controls these movements through the spinal motor neurons, which serve as the final common pathway to the muscles[2]. While the anatomical and physiological components of this system are well characterized[3], the overarching organisational principles that generate behaviours remain poorly understood. Here we elucidate the interplay between the anatomical structure of the musculoskeletal system and the functional organisation of distributed neural circuitry from which motor behaviours emerge.

The idea that the cortex controls muscles in a one-to-one fashion remains a dominant view in neuroscience, but several lines of evidence challenge this basic concept of motor control[4]. For example, it is widely recognized that the large degrees-of-freedom (DOFs) of the musculoskeletal system prohibits a simple one-to-one correspondence between a motor task and a particular motor solution. The combinatorial complexity of selecting a particular motor solution for every action makes it unlikely that the nervous system controls individual muscles in isolation; rather muscles are coupled and controlled in conjunction[5]. A coupling between muscles – whether mechanical or neural – constrains the number of effective DOFs and hence the number of potential movement patterns. This coupling thereby reduces the complexity of motor control[6, 7].

There is continuing debate about the nature of the coupling between muscles. The mechanical coupling in the musculoskeletal system constrains the movement patterns that can be generated[8, 9]. For example, correlations between joint angles confine the changes in musculotendon length to a low-dimensional subspace, resulting in correlated afferent inputs to spinal motor neurons[10]. The coupling between muscles could also result from the neural circuitry that drive spinal motor neurons[11]. Electrophysiological studies reveal that a combination of only a few coherent muscle activation patterns – or muscle synergies – can generate a wide variety of natural movements[12, 13]. Some of these patterns are already present from birth and do not

change during development and others are learned[14]. This supports the notion that the neuromuscular system has a modular organisation that simplifies the control problem[15, 16]. Spinal circuitry consisting of a network of premotor interneurons and motor neurons may mediate these synergistic drives to multiple muscles needed to generate basic movement patterns[17, 18]. Stimulation of interneuronal regions in the spinal cord show that these microcircuits are organised into discrete modules, each generating a specific pattern of muscular forces[19, 20]. These spinal networks may encode coordinated motor output programs[21], which can be used to translate descending commands for multi-joint movements into the appropriate coordinated muscle synergies that underpin those movements[3].

Network analysis can provide novel insights into the modular organisation of the musculoskeletal system. One of the most relevant features of complex networks is the community or modular structure[22, 23]. The investigation of the community structure of complex networks has been widely used in different domains such as metabolic[24] and brain networks[25]. Network analysis has recently been applied to investigate the structure and function of the musculoskeletal system: The anatomical network can be constructed by mapping the origin and insertion of muscles[26, 27] and we have shown how functional muscle networks can be constructed by assessing statistical dependencies – functional connectivity analysis – of surface electromyography (EMG) recorded from different muscles[28]. These functional networks reveal connectivity between groups of muscles at multiple frequency bands, resulting from correlated neural inputs to spinal motor neurons[29]. By using the same framework to characterise anatomical and neural connections between muscles, network analysis may elucidate the structure-function relationship of the human musculoskeletal system.

Here we investigate the organisational principles governing human motor control by comparing the community structure of anatomical and functional networks while participants performed postural tasks. We use multiplex modularity analysis [30] to assess the community structure of functional muscle networks across frequencies and task conditions. As biomechanical properties of musculoskeletal system constrain the movement patterns that can be generated, we anticipate a similar community structure for anatomical and functional muscles networks. Deviations in community structure

indicate additional constraints imposed by the central nervous system. We also compare functional connectivity between modules during different tasks conditions to investigate the reorganisation of muscle networks during behaviour. While average functional connectivity is constrained by anatomical constrains, we expect that functional muscle networks reconfigure to enable task-dependent coordination patterns between muscles. Such task modulations would indicate that functional interactions between muscles are not hard-wired, but are instead governed by dynamic connectivity in the central nervous system that is shaped by the anatomical topology of the musculoskeletal system.

Results

We assessed the relationship between anatomical and functional connectivity of 36 muscles distributed throughout the human body. Anatomical muscle networks were defined by mapping the physical connections between muscles and bones [26], which form a bipartite network[27]. Here we investigate a muscle-centric network in which the muscles represent the nodes and the attachments of muscles onto bones and cartilages the edges of the network. The structural connections were based on the international standard on human anatomical terminology[1]. This anatomical system constituted a densely connected, symmetrical network (Fig. 1; network density is 0.27). Modularity analysis revealed five modules that divided the anatomical muscle network into the main body segments (right arm, left arm, torso, right leg and left leg) with a modularity of 0.38.

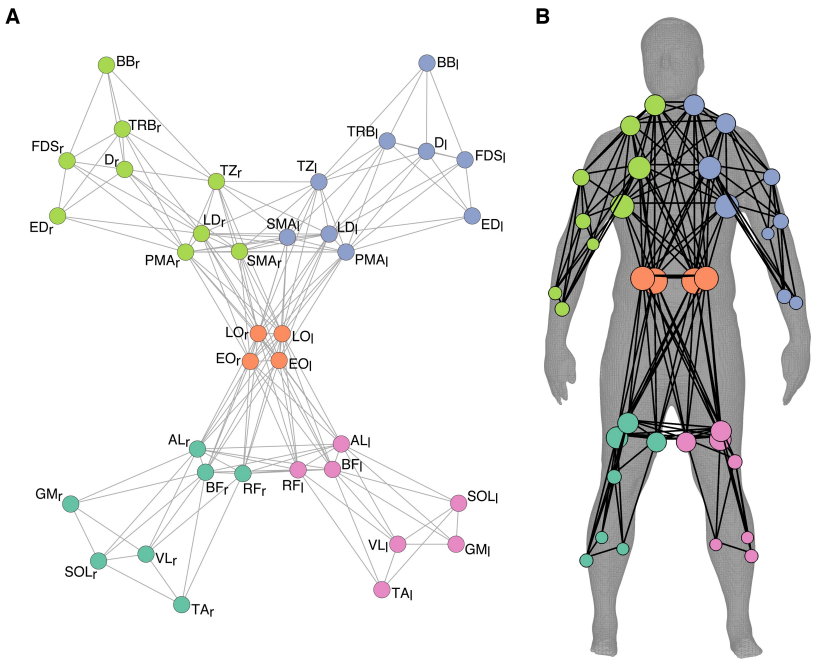

Figure 1. Community structure of the anatomical muscle network. A) Topological representation of the anatomical network. The muscles are the nodes of the network and edges represent anatomical connections between muscles that are attached to the same bones and cartilages. The five modules are color-coded. **B)** Spatial representation of anatomical muscle network displayed on human body[31]. The size of the nodes represents its degree.

Functional muscle networks were defined by mapping the neural interactions between muscles. To map functional networks, we measured EMG from these 36 muscles while healthy participants performed different postural tasks. A full factorial design was used in which we varied postural control (normal standing, instability in anterior-posterior or medial-lateral direction) and pointing behaviour (no pointing, pointing with the dominant hand or with both hands; see Methods for details). We assessed functional connectivity by means of intermuscular coherence between all muscle combinations and used non-negative matrix factorisation (NNMF) to decompose these coherence spectra into frequency components and corresponding edge weights. This yielded a set of weighted networks with their corresponding spectral fingerprints (frequency components).

We observed four separate frequency components (component 1: 0-3 Hz, component 2: 3-11 Hz, component 3: 11-21 Hz, component 4: 21-60 Hz; Fig. 2A), which serve as separate layers of a multiplex network. Weights were thresholded to obtain a minimally

connected binary network across layers and to keep the number of edges constant across layers (relative threshold of 0.035). Using multiplex modularity analysis, we obtained a fixed community structure across all four frequencies and nine conditions, which revealed six modules: right upper arm (rUA), bilateral forearms (FA), torso (T), right upper leg (rUL), left upper leg (lUL) and bilateral lower legs (LL) (Fig. 2B). Figure 2C depicts how these modules are distributed across the body. Distinct network topologies were observed across layers with a more widely connected network at lower frequencies and more partitioned network at higher frequencies: network density was 0.10, 0.09, 0.08, and 0.06 for components 1 to 4, respectively (Fig. 2D).

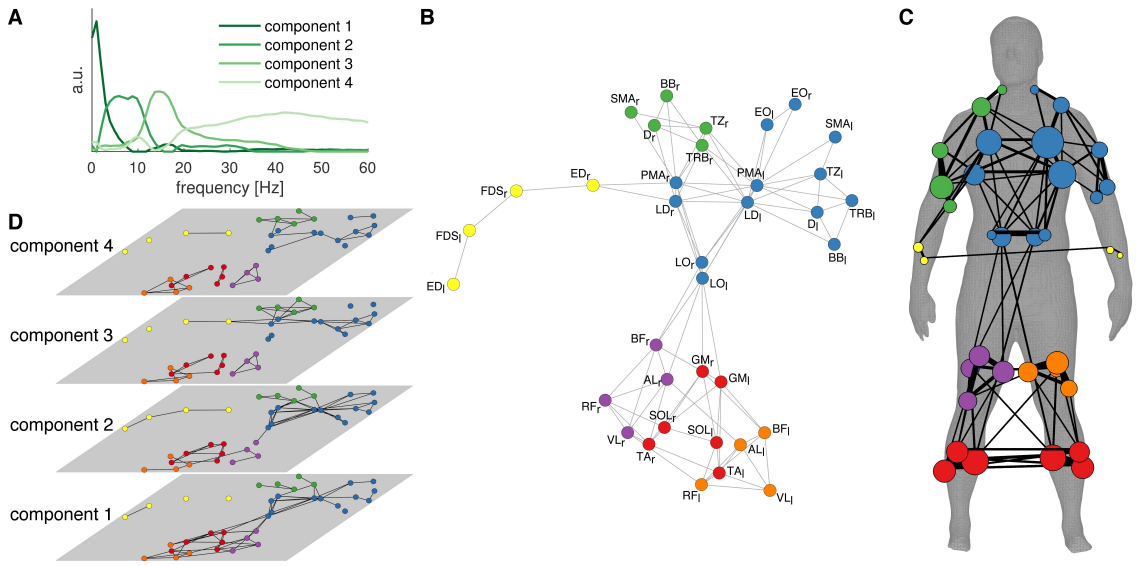

Figure 2. Community structure of multiplex functional muscle networks. A) The frequency spectra of the four components obtained using NNMF. **B)** Multiplex community structure of functional muscle network across layers and conditions. The dominant hand of all participants is displayed on the right side of the human body. **C)** Spatial representation of the average muscle network displayed on the human body[31]. The size of the nodes represents its degree and the width of the edges the average weight. **D)** The binary muscle networks for each layer.

The community structures of the anatomical and functional muscle networks were very similar (Rand index = 0.80, adjusted Rand index = 0.36, $P < 0.001$). A marked difference between anatomical and functional networks are the bilateral connections between homologous forearm and lower leg muscles in the functional networks, which were absent in the anatomical network. This is reflected in the community structure of the

functional networks, where bilateral lower leg muscles and bilateral forearm muscles were grouped in modules.

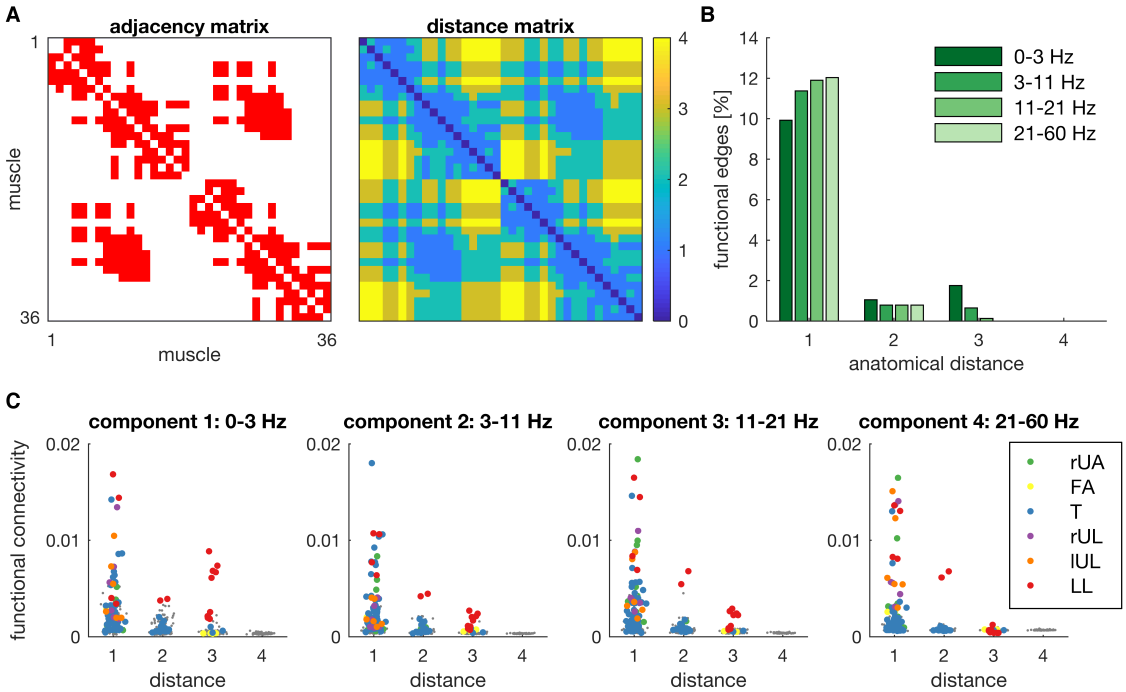

Figure 3. Relationship between functional connectivity and anatomical distance. A) Adjacency and distance matrix of the anatomical muscle network. Maximum path length is 4. **B)** Percentage of functional edges of thresholded networks across experimental conditions as a function of anatomical distance. **C)** Distribution of weights of functional networks as a function of anatomical distance for each layer. Weights were averaged across experimental conditions. Edges connecting muscles within the same module are color-coded (rUA: right upper arm, FA: bilateral forearms, T: torso, rUL: right upper leg, lUL: left upper leg, and LL: bilateral lower legs).

The relationship between anatomical distance (path length) and functional connectivity becomes apparent in Figure 3A. We first examined the percentage of all possible edges, i.e. the number of edges above threshold, which decreased as a function of anatomical distance: 11.3%, 0.9%, 0.6% and 0.0% for anatomical distance 1 to 4, respectively. This decline with distance was even more pronounced for the higher frequency components (Fig. 3B). Next, we examined the distribution of functional weights as a function of anatomical distance. The highest weights were observed for edges connecting muscles within the same module. The edges within most modules (rUA, T, rUL and lUL) had an anatomical distance of 1 and only a few edges within the FA and LL modules had an

anatomical distance of 2 or 3. In particular, edges connecting bilateral lower leg muscles (LL) showed relative large weights at an anatomical distance of 3 (Fig. 3C).

We next sought to study the influence of task on this structure-function relationship. This was achieved by employing clustered graphs to compare functional muscle networks across task conditions. The functional modules identified using the preceding multiplex modularity analysis form the nodes of these clustered graphs. Figure 4A shows the clustered graphs in the nine experimental conditions and for the four layers. The clustered graphs were very sparse, as modules have dense within module connections but sparse connections between nodes in other modules. Most edges were observed between leg muscles modules (LL, rUL and lUL) at the lowest frequency components (0-3 and 3-11 Hz), in particular when postural balance was challenged by instability in anterior-posterior or medial-lateral direction. Edges between the arm muscle modules (rUA and FA) and the torso (T) were mainly observed at the higher frequency components (11-21 and 21-60 Hz) during pointing (unimanual and bimanual).

The effects of the postural tasks were largely confined to the leg modules (Fig. 4C). Increased connectivity was observed during postural instability (anterior-posterior and medial-lateral) compared to normal standing across most frequency components. At the lowest frequency component (0-3 Hz), connectivity increased within and between most leg modules. Only small differences were observed at 3-11 Hz: increased connectivity between the torso (T) and lower leg (LL) modules during anterior-posterior instability and decreased connectivity within the torso module during medial-lateral instability. Connectivity increased again at the highest frequency components (11-21 and 21-60 Hz) within and between the torso and leg modules (rUL, lUL, and LL).

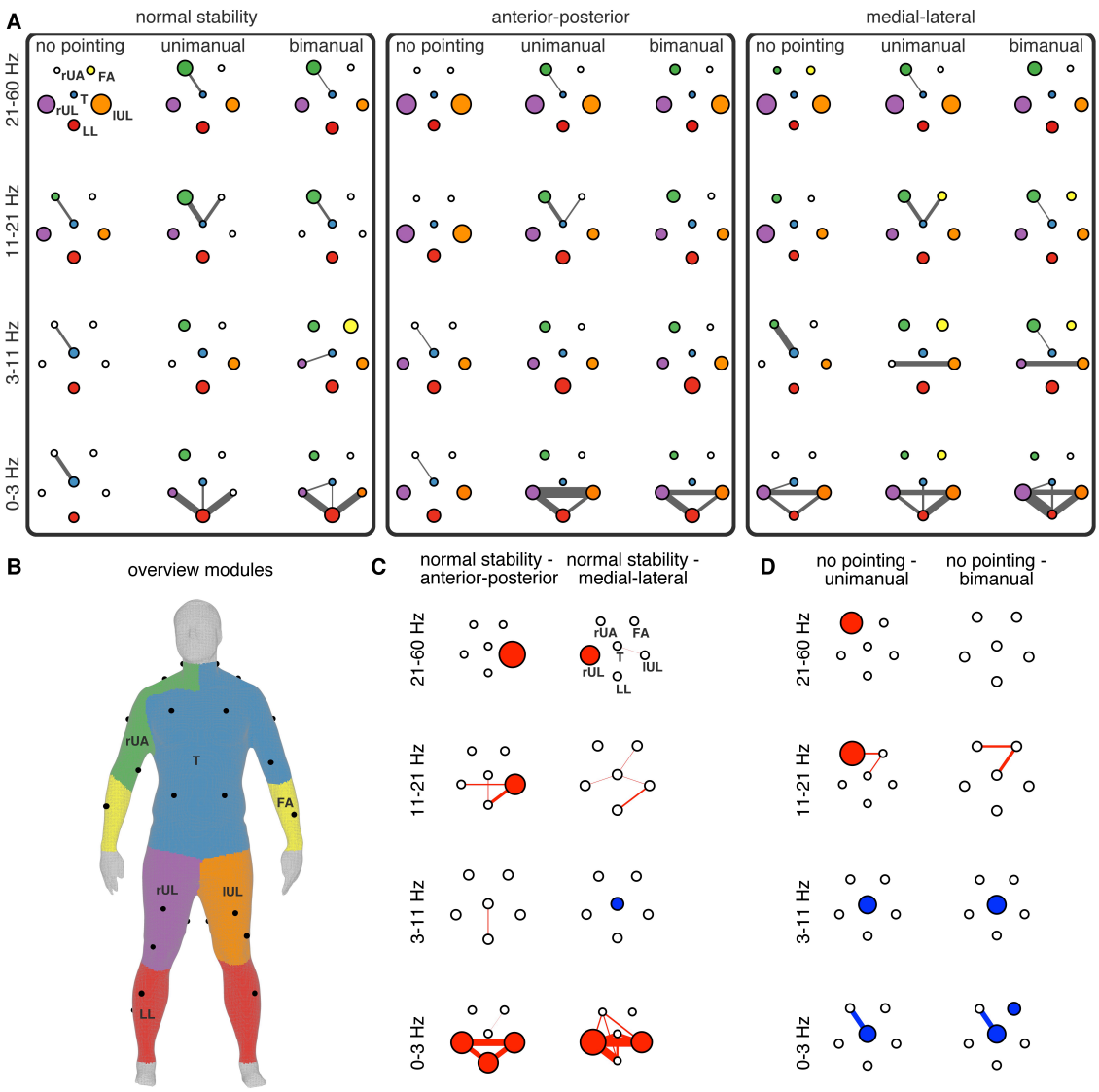

Figure 4. Clustered graphs of functional muscle networks across conditions. A) The clustered graphs in the nine experimental conditions (columns) and for every layer (rows). The nodes are the modules identified using multiplex modularity analysis. Node size represents the network density within and the width of the edges the connection density between modules. **B)** Spatial representation of the functional modules on the human body: right upper arm (rUA), bilateral forearms (FA), torso (T), right upper leg (rUL), left upper leg (lUL) and bilateral lower legs (LL). We used the Matlab toolbox for geometry processing to generate the coloured meshes[32]. **C)** Significant differences in clustered graphs between the stability conditions. Two contrasts were assessed: normal stability – anterior-posterior instability and normal stability – medial-lateral instability. A permutation test was used with a significance threshold corrected for multiple comparisons ($P < 0.0033$). Significant differences are color-coded: Red depicts an increase and blue a decrease in the average weights. **D)** Significant differences in clustered graphs between the pointing conditions. Two contrasts were assessed: no pointing – unimanual pointing and no pointing – bimanual pointing.

The pointing tasks showed a different pattern compared to the postural tasks, but the effects of unimanual and bimanual pointing were very similar (Fig. 4D). During pointing, connectivity decreased within the torso (T) module at the lowest frequency components (0-3 and 3-11 Hz) and between the torso and the right upper arm (rUA) module only at the lowest frequency component (0-3 Hz). In contrast, a significant increase in connectivity within the rUA module was observed during unimanual point compared to no pointing at the highest frequency components (11-21 and 21-60 Hz). In addition, there was increased connectivity between the torso and the forearm (FA) modules and between rUA and FA during pointing (unimanual and bimanual) compared to no pointing at frequency component 3 (11-21 Hz).

Discussion

We used a network approach to study the structure-function relationship of the human musculoskeletal system. Several principles of the functional relationship between muscles were uncovered: (i) Functional connectivity patterns between muscles are strongly shaped by the anatomical constraints of the musculoskeletal system, with functional connectivity strongest within anatomical modules and decreased as a function of anatomical distance; (ii) Bilateral connectivity between the homologous upper and lower extremities is a key characteristic of the functional muscle networks; (iii) The functional relationships are state-dependent with postural tasks differentially impacting upon functional connectivity at different frequency ranges. The use of a multiplex approach allows the integration of functional muscle networks across frequencies and provides a unique unifying window into the distributed circuitry of the human central nervous system that controls movements.

Identifying relationships between anatomical and functional muscle networks is crucial for understanding how movement is coordinated. Previous studies either investigated how biomechanical properties of the musculoskeletal system constrain the movement patterns that can be generated[9, 10], or how muscle activation patterns can be explained by a combination of only a few coherent muscle activation patterns[12, 13]. Our combined analyses of anatomical and functional muscle networks reveal a strong relationship between muscle activation patterns and the anatomical connections in the musculoskeletal systems. This agrees with previous research showing that common

input is strongest to spinal motor neurons that innervate muscles pairs that are anatomically and functionally closely related[11, 33]. These findings support the notion that the anatomical embedding of muscles in the skeletal system results in correlated (low-dimensional) muscle activity patterns.

The musculoskeletal properties of the human body restrict the postural dynamics and constrain changes in musculotendon length across joints[10]. These mechanical couplings result in correlated proprioceptive feedback and hence in correlated input to spinal motor neurons. Sensory afferents can generate correlated input to different pools of motor neurons through direct afferent pathways – the monosynaptic reflex arc – or via spinal interneurons that mediate efferent motor commands [3, 34]. The influence of biomechanics on functional muscle networks is expected to be most pronounced at the lower frequency components, as muscles act as a low pass filter of neuronal inputs[35]. The similarity in community structure of anatomical and functional networks may also result from a somatotopic organisation of the neural motor system. Interestingly, the community structure of the anatomical muscle network mirrors the organisation of primary motor cortex control modules[27]. Likewise, the spatial organisation of motor neurons of the spinal cord is also related to the anatomical organisation of muscles[36]. The topographic organisation of spinal motor neurons is similar across species[37] and may hence be a result of evolutionary conservation[38]. The similarity between structural and functional networks has been a signature of the study of brain networks[39] and the topology of brain networks depends on the brain's spatial embedding[40, 41]. The present findings suggest that the principles governing embodied structural and functional networks also applies to the neural circuitry that controls movements and may hence reflect a general principle of the central nervous system.

Bilateral modules consisting of the upper and lower extremities are a key characteristic of the functional muscle network that is absent in the anatomical network. The two bilateral forearm muscles (FDS and ED) were grouped into the same module and showed coupling predominantly in the 3-11 Hz frequency component. This is consistent with previous studies showing bimanual coupling at ~10 Hz between homologous hand and forearm muscles[42, 43]. The bilateral forearm muscles were only weakly coupled to other muscles and were thus on the periphery of functional muscle network (Fig. 2).

This may reflect the relatively high proportion of direct monosynaptic corticospinal projections – and thus a relative low proportion of diverging projections – to motor neurons innervating hand and forearm muscles needed for the control of independent finger movements[44]. The observed bimanual coupling at 3-11 Hz may be generated by the olivocerebellar system, which is known to produce oscillations in this frequency range and for its involvement in the formation of muscles in functional muscle collectives[43, 45]. In contrast, the bimanual module of lower leg muscles revealed strong coupling at multiple frequency bands, consistent with previous analyses on functional muscle networks[28], and showed the strongest long-range connections observed in the present study (Fig. 3C). Bilateral connectivity between homologous muscles during balancing could be generated by the vestibulospinal tract, which is known to be involved in postural balance and innervate the spinal grey matter bilaterally[33]. Bilateral connectivity has been observed at all levels of the corticospinal axis[46] and is paramount for functional brain networks, particularly between homologous left-right cortical regions[47, 48]. The present findings suggest that bilateral coupling is also a defining feature of functional muscle networks.

Functional connectivity was not static but displayed clear task-dependent modulations. The observed changes were linked to the postural task the subjects performed: functional connectivity was increased within and between the leg modules during postural instability, and increased within and between arm and upper body modules in the pointing conditions. Functional connectivity between muscles is thus task dependent[33, 42, 49], suggesting the presence of multifunctional circuits in which a given anatomical connectivity pattern can generate different functional activity patterns under various conditions[34]. Such a distributed circuitry creates the substrate to support many behaviours that are driven by the concerted actions of a large distributed network as opposed to simple, dedicated pathways. The underlying network connectivity hence constrains the possible patterns of population activity to a low-dimensional manifold spanned by a few independent patterns – neural modes – that provide the basic building blocks of neural dynamics and motor control[50]. Again, this finds similarities with recent investigations of the functional principles of cognitive networks in the brain[51, 52].

Task-dependent changes occurred at different frequencies, which indicate the functioning of a multiplex network organisation, whereby the four frequency components reflect different types of interactions between muscles. Four distinct frequency components (0-3, 3-11, 11-21, and 21-60 Hz) were extracted from the coherence spectra using NNMF. These frequency bands closely match those found previously[28], demonstrating the robustness of this finding. An interesting possibility is that these frequency components reflect the spectral fingerprints of different pathways that project onto the spinal motor neurons. It has been suggested that these different frequencies may have specific roles in coding motor signals[53]. Functional connectivity at the lowest frequency components may result from afferent pathways, while functional connectivity at higher frequencies may reflect correlated input from descending pathways. For example, functional connectivity in the beta band (15-30 Hz) most likely reflects corticospinal projections[11, 42]. The highest frequency components observed in this study (21-60 Hz) showed the most local connectivity patterns. These local connectivity patterns may reflect propriospinal pathways[3, 21]. If layers of the functional muscle network signify different neural pathways, then these functional connectivity patterns may be used to uncover the contribution of these pathways in the formation of coordinated activity patterns in the motor system that are difficult to assess directly[29].

In summary, our network analysis revealed widespread functional connectivity between muscles, indicative of correlated inputs to spinal motor neurons at multiple frequencies. Correlated inputs indicate divergent projections or lateral connections in the neural pathways that innervate spinal motor neurons. These findings are consistent with many-to-many connectivity rather than a one-to-one mapping between brain and muscle[4]. Complex movements arise through relatively subtle changes in the co-activation of different distributed functional modes. We present a novel approach that aligns movement neuroscience with current research on brain and physiological networks by showing how the central nervous system interacts with the musculoskeletal system of the human body. From a systems biology perspective, the brain and spinal cord are interwoven with the body: they are 'embodied'[8]. Such an integrative framework – considering functional interactions between supra-spinal, spinal and peripheral regions simultaneously using network analysis – may provide new insights into neurological disorders[54].

Methods

Data acquisition

Fourteen healthy participants (seven males and seven females, mean age 25±8 years, ten right and four left handed) without any neurological, motor disorder or diabetes mellitus and with a BMI below 25 were included in this study. The experiments were approved by the Ethics Committee Human Movement Sciences of the Vrije Universiteit Amsterdam (reference ECB 2014-78) and performed in full compliance with the Declaration of Helsinki. All participants were written and verbally informed about the procedure and signed an informed consent prior to participation.

Participants were instructed to perform nine different postural tasks. A full factorial design was used in which postural control (normal standing, instability in anterior-posterior direction and instability in medial-lateral direction) and pointing behaviour (no pointing, pointing with dominant hand, pointing with both hands) were varied. Postural stability was manipulated using a balance board with one degree of freedom, which allows movement either in the anterior-posterior or medial-lateral direction. In the pointing task, participants held a laser pointer with their dominant hand (unimanual) or with both hands (bimanual) and pointed it on a white target (25 cm^2) located at a distance of 2.25 meter parallel to the transversal axis of the body at the height of the acromion of the participant. The experiment hence consisted of nine (3×3) experimental conditions. The duration of a trial was 30 seconds and each condition was repeated six times.

Bipolar surface EMG was recorded from 36 muscles distributed across the whole body, i.e. 18 bilateral muscles (Table 1). EMG was acquired using three 16-channel Porti systems (TMSi, Enschede, The Netherlands), online high-pass filtered at 5 Hz and sampled at 2 kHz.

Table 1. List of muscles

Muscle	Abbreviation
tibialis anterior	TA
gastrocnemius medialis	GM
soleus	SOL
rectus femoris	RF
biceps femoris	BF
vastus lateralis	VL
adductor longus	AL
external oblique	EO
pectoralis major	PMA
sternocleidomastoideus	SMA
longissimus	LO
latissimus dorsi	LD
trapezius	TZ
deltoid	D
biceps brachii	BB
triceps brachii	TRB
extensor digitorum	ED
flexor digitorum superficialis	FDS

Anatomical muscle network

The anatomical muscle network was defined by mapping the physical interactions between muscles[26]. The 36 muscles (18 left and 18 right) represent the nodes and the tendinous attachments of muscles onto bones and cartilages form the edges of the network. The structural connections were based on the international standard on human anatomical terminology[1]. Bones that show no or almost no motion in the joint between them were considered as one rigid bony structure, i.e. the pelvis, skeleton thoracis or ossa cranii. The connections between muscles and bones listed in Table 2 denote a bipartite network C with muscles as one group and bones as the second group. We then created a muscle-centric network as the one-mode projections of C: $B = CC^T$[27]. This gave a weighted adjacency matrix where the weights reflect the number of bones by which two muscles are connected. We converted this to a binary network by setting all weights to 1.

Table 2. Origin and insertion of muscles

Muscle	Origin 1	Origin 2	Origin 3	Insertion 1	Insertion 2
TA	tibia			os cuneiforme mediale	ossa metatarsi
GM	femur			calcaneus	
SOL	fibula	tibia		calcaneus	
RF	os coxae[1,*]	os ilium[1,*]		tibia	
BF	femur	os ischii[1,*]		fibula	tibia
VL	femur			tibia	
AL	os pubis[1,*]			femur	
EO	costae[2,*]			linea alba	os ilium[1,*]
PMA	clavicula	costae[2,*]	sternum[2,*]	humerus	
SMA	clavicula	sternum[2,*]		os temporale[3,*]	
LO	ligamentum sacrospinale[1,*]	vertebra[*]		costae[2,*]	vertebra[*]
LD	costae[2,*]	fascia thoracolumbalis[*]	vertebra[*]	humerus	
TZ	ligamentum nuchae[*]	os occipitale[3,*]	vertebra[*]	clavicula	scapula
D	clavicula	scapula		humerus	
BB	scapula			radius	
TRB	humerus	scapula		ulna	
ED	humerus			ossa digitorum	
FDS	humerus	radius	ulna	ossa digitorum	

[1] Part of the pelvis; [2] Part of the skeleton thoracis; [3] Part of the ossa cranii; [*] Connective structure on the midline of the body connecting bilateral muscles

Functional muscle networks

EMG was filtered offline with a band-pass filter (1-400 Hz) before independent component analysis was used for electrocardiography removal[55]. For each participant, one or two independent components were removed. EMG data was then high-pass filtered (20 Hz) and EMG envelopes were extracted by means of the Hilbert amplitude[56].

We followed the procedure described in Boonstra et al.[28] to extract functional muscle networks from surface EMG. First, complex-valued coherency was estimated and averaged over trials within each condition for each participant. The absolute value of coherency was squared to obtain magnitude-squared coherence. Intermuscular coherence was assessed between all 630 muscle pairs. Next, non-negative matrix factorisation (NNMF)[57] was used to decompose these coherence spectra across all conditions and participants into four distinct frequency components and the corresponding weights. This yielded an undirected weighted network for each frequency component.

These functional networks were converted to binary networks to facilitate comparison to the anatomical network. Weights were thresholded to obtain a minimally connected

network across conditions and frequency components, which corresponded to a relative threshold of 0.035. This resulted in sparse networks in which each node was connected to at least one other node by an edge at one of the layers of the multiplex network. Stringent thresholding is required to maintain the key properties of weighted networks, as specificity is as important as sensitivity to the estimation of network topology[58].

Community structure

The standard Louvain algorithm was used to extract the modules from the anatomical networks[59]. As the Louvain algorithm is stochastic, we used consensus clustering to obtain a stable partition across 1000 iterations[60]. Multiplex modularity analysis[30] was used to identify the modules of functional muscle network across the conditions and frequency components. We used *MolTi*, a standalone graphical software, to detect communities from multiplex networks by optimising the multiplex-modularity with the adapted Louvain algorithm (https://github.com/gilles-didier/MolTi). Modules were extracted across the 36 (9×4) binary networks, as multi-graph approaches can improve clustering accuracy[61]. The resolution for the modularity analysis was set to 1. We used the Rand index and the adjusted Rand index to compare the modules of the anatomical and functional muscle networks[23].

Comparison of functional networks across conditions

To facilitate the comparison of functional networks across task conditions, we coarse-grained the networks[62]. We used the set of functional modules estimated across conditions and frequency components as a frame of reference to coarse-grain the 36 binary networks and then compared the strength of the inter- and intra-module connections across networks using these module boundaries. In the clustered networks the nodes are the modules (group of muscles, identified above) and the edges represent the average connection strength between the modules. The non-diagonal elements of the resulting weighted adjacency matrix represent the average number of links between two modules and diagonal elements the average number of links within a module.

To compare the clustered networks across conditions, we used simple contrasts between conditions and quantified differences in the numbers of connections between

and within modules. To test the statistical significance of these contrast, we performed paired permutation tests separately on each of the matrix elements[62]. The clustered networks had a much-reduced dimensionality compared to the original functional muscle networks. Family-wise error control was maintained using Bonferroni correction ($P<0.0033$) to correct for multiple comparisons.

References

1. Berkovitz B, Heimer L, Henkel C, Ma T, McNeal J, Moore N. Terminologia Anatomica: International Anatomical Terminology (Fcat). New York: Thieme Stuttgart (1998).
2. Sherrington C. *The integrative action of the nervous system*. CUP Archive (1910).
3. Pierrot-Deseilligny E, Burke D. *The circuitry of the human spinal cord: its role in motor control and movement disorders*. Cambridge University Press (2005).
4. Graziano M. The organization of behavioral repertoire in motor cortex. *Annu Rev Neurosci* **29**, 105-134 (2006).
5. Bernstein N. *The coordination and regulation of movements*. Pergamon (1967).
6. Turvey MT. Coordination. *Am Psychol* **45**, 938-953 (1990).
7. Kelso JS. *Dynamic patterns: The self-organization of brain and behavior*. MIT press (1997).
8. Chiel HJ, Beer RD. The brain has a body: adaptive behavior emerges from interactions of nervous system, body and environment. *Trends Neurosci* **20**, 553-557 (1997).
9. Kuo AD, Zajac FE. Human standing posture: multi-joint movement strategies based on biomechanical constraints. *Progr Brain Res* **97**, 349-358 (1993).
10. Kutch JJ, Valero-Cuevas FJ. Challenges and new approaches to proving the existence of muscle synergies of neural origin. *PLoS Comput Biol* **8**, e1002434 (2012).
11. Farmer SF, Bremner FD, Halliday DM, Rosenberg JR, Stephens JA. The frequency content of common synaptic inputs to motoneurones studied during voluntary isometric contraction in man. *J Physiol* **470**, 127-155 (1993).
12. d'Avella A, Saltiel P, Bizzi E. Combinations of muscle synergies in the construction of a natural motor behavior. *Nat Neurosci* **6**, 300-308 (2003).
13. Ting LH, Macpherson JM. A limited set of muscle synergies for force control during a postural task. *J Neurophysiol* **93**, 609-613 (2005).
14. Dominici N, *et al.* Locomotor primitives in newborn babies and their development. *Science* **334**, 997-999 (2011).
15. Ghahramani Z, Wolpert DM. Modular decomposition in visuomotor learning. *Nature* **386**, 392 (1997).
16. Mussa-Ivaldi FA. Modular features of motor control and learning. *Curr Opin Neurobiol* **9**, 713-717 (1999).
17. Giszter SF. Motor primitives—new data and future questions. *Curr Opin Neurobiol* **33**, 156-165 (2015).
18. Takei T, Confais J, Tomatsu S, Oya T, Seki K. Neural basis for hand muscle synergies in the primate spinal cord. *Proc Nat Acad Sci* **114**, 8643-8648 (2017).
19. Tresch MC, Saltiel P, Bizzi E. The construction of movement by the spinal cord. *Nat Neurosci* **2**, 162-167 (1999).
20. Hart CB, Giszter SF. A neural basis for motor primitives in the spinal cord. *J Neurosci* **30**, 1322-1336 (2010).
21. Levine AJ, *et al.* Identification of a cellular node for motor control pathways. *Nat Neurosci* **17**, 586 (2014).
22. Newman ME. Modularity and community structure in networks. *Proc Nat Acad Sci* **103**, 8577-8582 (2006).
23. Fortunato S. Community detection in graphs. *Phys Rep* **486**, 75-174 (2010).
24. Ravasz E, Somera AL, Mongru DA, Oltvai ZN, Barabási AL. Hierarchical organization of modularity in metabolic networks. *Science* **297**, 1551-1555 (2002).
25. Bullmore E, Sporns O. Complex brain networks: graph theoretical analysis of structural and functional systems. *Nat Rev Neurosci* **10**, 186-198 (2009).
26. Esteve-Altava B, Diogo R, Smith C, Boughner JC, Rasskin-Gutman D. Anatomical networks reveal the musculoskeletal modularity of the human head. *Sci Rep* **5**, 8298 (2015).
27. Murphy AC, *et al.* Structure, function, and control of the musculoskeletal network. *arXiv:161206336* (2016).

28. Boonstra TW, Danna-Dos-Santos A, Xie HB, Roerdink M, Stins JF, Breakspear M. Muscle networks: Connectivity analysis of EMG activity during postural control. *Sci Rep* **5**, 17830 (2015).
29. Boonstra TW, Farmer SF, Breakspear M. Using computational neuroscience to define common input to spinal motor neurons. *Front Hum Neurosci* **10**, 313 (2016).
30. Didier G, Brun C, Baudot A. Identifying communities from multiplex biological networks. *PeerJ* **3**, e1525 (2015).
31. Makarov SN, Noetscher GM, Nazarian A. Triangular surface human body meshes for computational purposes. In: *Low-Frequency Electromagnetic Modeling for Electrical and Biological Systems Using MATLAB*. Wiley (2015).
32. Jacobson A. Matlab toolbox for Geometry Processing. *GitHub Repository*, https://github.com/alecjacobson/gptoolbox (2017).
33. Gibbs J, Harrison LM, Stephens JA. Organization of inputs to motoneuron pools in man. *J Physiol* **485**, 245-256 (1995).
34. Briggman K, Kristan Jr W. Multifunctional pattern-generating circuits. *Annu Rev Neurosci* **31**, 271-294 (2008).
35. Partridge LD. Signal-handling characteristics of load-moving skeletal muscle. *Am J Physiol* **210**, 1178-1191 (1966).
36. Bácskai T, Fu Y, Sengul G, Rusznák Z, Paxinos G, Watson C. Musculotopic organization of the motor neurons supplying forelimb and shoulder girdle muscles in the mouse. *Brain Struct Funct* **218**, 221-238 (2013).
37. McHanwell S, Biscoe T. The localization of motoneurons supplying the hindlimb muscles of the mouse. *Phil Trans R Soc B* **293**, 477-508 (1981).
38. Lacquaniti F, Ivanenko YP, D'avella A, Zelik K, Zago M. Evolutionary and developmental modules. *Front Comp Neurosci* **7**, 61 (2013).
39. Honey CJ, Kötter R, Breakspear M, Sporns O. Network structure of cerebral cortex shapes functional connectivity on multiple time scales. *Proc Nat Acad Sci* **104**, 10240-10245 (2007).
40. Roberts JA*, et al.* The contribution of geometry to the human connectome. *NeuroImage* **124**, 379-393 (2016).
41. Horvát S*, et al.* Spatial embedding and wiring cost constrain the functional layout of the cortical network of rodents and primates. *PLoS Biol* **14**, e1002512 (2016).
42. De Vries IEJ, Daffertshofer A, Stegeman DF, Boonstra TW. Functional connectivity in neuromuscular system underlying bimanual coordination. *J Neurophysiol* **116**, 2576-2585 (2016).
43. McAuley JH, Farmer SF, Rothwell JC, Marsden CD. Common 3 and 10 Hz oscillations modulate human eye and finger movements while they simultaneously track a visual target. *J Physiol* **515**, 905-917 (1999).
44. Lemon RN. Descending pathways in motor control. *Annu Rev Neurosci* **31**, 195-218 (2008).
45. Welsh JP, Llinás R. Some organizing principles for the control of movement based on olivocerebellar physiology. *Progr Brain Res* **114**, 449-461 (1997).
46. Carson R. Neural pathways mediating bilateral interactions between the upper limbs. *Brain Res Rev* **49**, 641-662 (2005).
47. Biswal B, Zerrin Yetkin F, Haughton VM, Hyde JS. Functional connectivity in the motor cortex of resting human brain using echoplanar MRI. *Magn Reson Med* **34**, 537-541 (1995).
48. Shen K*, et al.* Stable long-range interhemispheric coordination is supported by direct anatomical projections. *Proc Nat Acad Sci* **112**, 6473-6478 (2015).
49. Laine CM, Martinez-Valdes E, Falla D, Mayer F, Farina D. Motor neuron pools of synergistic thigh muscles share most of their synaptic input. *J Neurosci* **35**, 12207-12216 (2015).
50. Gallego JA, Perich MG, Miller LE, Solla SA. Neural manifolds for the control of movement. *Neuron* **94**, 978-984 (2017).

51. Cole MW, Bassett DS, Power JD, Braver TS, Petersen SE. Intrinsic and task-evoked network architectures of the human brain. *Neuron* **83**, 238-251 (2014).
52. van den Heuvel MP, Sporns O. Network hubs in the human brain. *Trends Cog Sci* **17**, 683-696 (2013).
53. McAuley JH, Marsden CD. Physiological and pathological tremors and rhythmic central motor control. *Brain* **123**, 1545-1567 (2000).
54. Freund P*, et al.* Embodied neurology: an integrative framework for neurological disorders. *Brain* **139**, 1855-1861 (2016).
55. Willigenburg NW, Daffertshofer A, Kingma I, van Dieen JH. Removing ECG contamination from EMG recordings: a comparison of ICA-based and other filtering procedures. *J Electromyogr Kinesiol* **22**, 485-493 (2012).
56. Boonstra TW, Breakspear M. Neural mechanisms of intermuscular coherence: implications for the rectification of surface electromyography. *J Neurophysiol* **107**, 796-807 (2012).
57. Lee DD, Seung HS. Learning the parts of objects by non-negative matrix factorization. *Nature* **401**, 788-791 (1999).
58. Zalesky A, Fornito A, Cocchi L, Gollo LL, van den Heuvel MP, Breakspear M. Connectome sensitivity or specificity: which is more important? *Neuroimage* **142**, 407-420 (2016).
59. Blondel VD, Guillaume J-L, Lambiotte R, Lefebvre E. Fast unfolding of communities in large networks. *J Stat Mech Theor Exp* **2008**, P10008 (2008).
60. Lancichinetti A, Fortunato S. Consensus clustering in complex networks. *Sci Rep* **2**, 336 (2012).
61. Papalexakis EE, Akoglu L, Ience D. Do more views of a graph help? community detection and clustering in multi-graphs. In: *Information fusion (FUSION), 2013 16th international conference on* (2013).
62. Kujala R, Glerean E, Pan RK, Jääskeläinen IP, Sams M, Saramäki J. Graph coarse-graining reveals differences in the module-level structure of functional brain networks. *Eur J Neurosci* **44**, 2673-2684 (2016).